Period Analysis, Photometry, and Astrophysical Models of the Eclipsing Binary TW Crucis

David J. W. Moriarty
315 Main Road, Wellington Point, Qld. 4160, Australia and School of Mathematics and Physics, The University of Queensland, Qld 4072, Australia; djwmoriarty@bigpond.com

Received July 27, 2015; revised August 20, 2015; accepted September 1, 2015

Abstract TW Crucis is a W-type W UMa contact eclipsing binary that has not been studied in detail since discovery in 1926. During 5 seasons from 2011 to 2015, photometric CCD observations were obtained mostly in the V passband, but also some in B and I passbands. The period was found to be 0.3881444 ± 0.0000006 day, which is not substantially different from the original period of 0.3881358 day. There were slight variations in the period from cycle to cycle and year to year, which are most likely due to asymmetry in the light curves caused by star spots. A preliminary model of the light curves indicates the mass ratio may be about 0.67, inclination 70.8°, and fillout factor 0.11. As no spectra are available, the range in B–V and V–I color indices of 0.8–0.87 and 0.87–0.92, respectively, were used to estimate the effective temperatures for the modelling, based on the spectral types of K0–K2. The spectral type may be earlier, if the color indices are affected by interstellar reddening. Star spots, which changed over short period cycles and were required to obtain good fits of the models to the light curves, indicate the stars are magnetically active.

1. Introduction

The formation and evolution of short period contact binary stars is not well understood. Pribulla and Rucinski (2006) comment that those with periods of less than 1 day should not exist, and suggest they may have formed in triple or larger multiple systems. They applied several methods to examine whether contact eclipsing binary systems brighter than Vmax = 10 might have a third component and commented their statistical analysis was limited by the paucity of data from the southern hemisphere as well as for fainter systems generally. A third component would be apparent from cyclic or sinusoidal variations in the period, which would be detected by comparing observed times of minimum with times calculated from an ephemeris. Small apparent cycle-to-cycle variations in the period of eclipsing binaries have been discussed recently by Mohajerani and Percy (2015), who offered several explanations, including the effect of star spots and the presence of a third star. The W Ursae Majoris contact eclipsing binaries have been divided into two classes: the A type, in which the more massive and brighter component is the hotter star, and the W type, in which the more massive and brighter component is the cooler star (Binnendijk 1970). Thus the primary eclipse in A-type systems is a transit, whereas in W-type systems, the primary eclipse is an occultation of the smaller, hotter star.

TW Crucis is a W-type W UMa-type contact eclipsing binary that was discovered in 1926 by Bruna (1930), who determined a period of 0.3881358 ± 0.000002 day. It has not been studied in detail since then other than as part of the All Sky Automated Survey (ASAS), which has provided data to update the period to 0.388149 day (Pojmański 2002). A similar period of 0.38814626 day was reported by Kreiner (2004). In the work reported here, the aims were to check times of minima to determine whether there were any changes in the period and to develop a preliminary model of the system with photometric data from full light curves in B, V, and I passbands.

2. Methods, observations, and analysis

The instruments used for photometry were a 280-mm Celestron Schmidt-Cassegrain with a SBIG ST8 charge-coupled device (CCD) camera with Johnson B and V and Ic filters, on a German Equatorial mount at Wellington Point, a coastal site. In 2014, a new observatory was established at Glen Aplin, a dark sky site at 750-m altitude, with a 356-mm Celestron Edge HD 1400 aplanatic Schmidt Cassegrain telescope on a Mathis Instruments fork mount and a Moravian G3-6303 CCD camera with Johnson B and V and Bessel I filters. As the initial aim was to determine whether there were period changes, the V filter only was used between 2011 and 2014. For a better understanding of the TW Cru system and to obtain color index values, the B and I filters were also used in 2015. However, as exposure times of 3 minutes were required for the B passband, cadences were lower than optimum for determining accurate times of minimum, and as cloudy weather intervened, the light curves in the B band were not of high quality.

The images were reduced using aperture photometry with MAXIMDL (Diffraction Limited 2012). Magnitudes were calibrated against the standard stars in the LSE 259, WD 1153-484, and MCT 2019-4339 sequences at about –50° declination (Landolt 2007). The instrumental magnitudes in two or three passbands were transformed to the standard system with spreadsheets in MICROSOFT EXCEL (Richards 2013, 2015). The computer clock was synchronized at 15-to-20 minute intervals with an NTP time server using DIMENSION 4 (Thinking Man Software 1992–2014).

The comparison star chosen for this work was GSC 08978-00019 (UCAC4: 136-071292), as it was close to the variable and had a similar magnitude and color indices (Table 1). The check star was TYC 8978 1844-1. The positions are marked on a portion of the AAVSO-VSP chart (Figure 1).

The times of minima and the magnitudes at minimum (phases 0 and 0.5) and maximum light (phases 0.25 and

Table 1. Magnitude and color indices of TW Cru, comparison, and check stars used in this work.

Star	*R. A. (2000)* *h m s*	*Dec. (2000)* *° m s*	*B*	*V*	*Ic*	*B–V*	*V–Ic*
GSC 08978-00019	12 03 00.14	–62 55 41.8	13.351	12.598	11.715	0.753	0.888
error			0.035	0.006	0.073	0.041	0.079
TYC 8978 1844-1	12 02 43.22	–62 52 30.3	12.448	11.98	11.362	0.468	0.618
error			—*	0.006	0.025	—	0.031
TW Cru	12 03 16.15	–62 56 15.6	13.22	12.452	11.538	0.768	0.914
error			0.028	0.006	0.032	0.034	0.038

**Error for B not available. Source: APASS DR7: Henden et al. (2013). The Ic magnitudes were calculated from the Sloan g and i values with the formula* $Ic = i - 0.3645 - 0.0743 \times (g - i) + 0.0037 \times (g - i)^2$ *(Munari et al. 2014).*

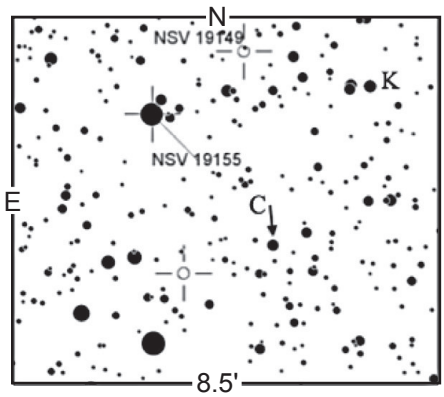

Figure 1. The central portion of the finder chart for TW Cru showing the comparison (C) indicated with the arrow and check (K) stars (https://www.aavso.org/apps/vsp/chart/X15281GC.png).

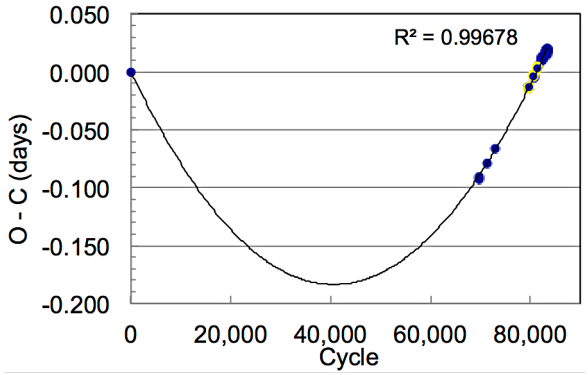

Figure 2. TW Cru (O–C) diagram for the period between 1926 and 2015, based on the original period and epoch. See Table 2 for details of epochs.

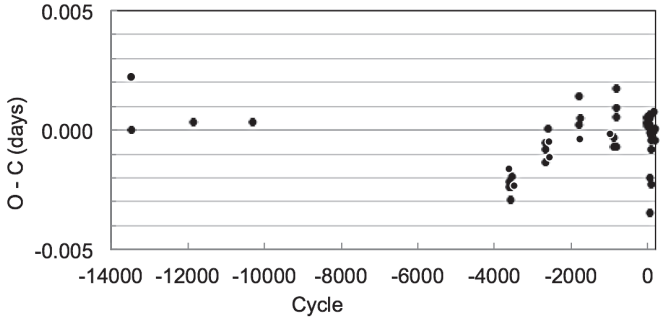

Figure 3. Variations in O–C values for primary and secondary minima between 2000 and 2015.

0.75) were determined using a 7-order polynomial fit in PERANSO (Vanmunster 2013). Phase-magnitude light curves were produced in PERANSO and exported for modelling. The procedures described in the BINARY MAKER 3 manual (Bradstreet and Steelman 2002) and by Bradstreet (2005) were used to determine models of the TW Cru system.

3. Results

3.1. Period analysis

In the 5 years between 2011 and 2015, 45 times of minimum were recorded (Table 2). A new ephemeris was determined from these data with a least squares linear regression (Equation 1). The epoch for this work was calculated from 96 data points around the primary minimum of HJD 2457101.1430, which was a night with good seeing; the total data set for that night, which included the secondary minimum, was 423 observations in the V passband.

$$\text{HJD (Min I)} = 2457101.1433\ (0.0002) + 0.3881444\ (0.0000006) \times E \quad (1)$$

A parabola can be fitted to the graph of the observed minus calculated epochs (O–C) between the original epoch determined by Bruna (1930) and cycle 83,463, the most recent in 2015 (Figure 2).

$$y = 1 \times 10^{-10}\, x^2 - 9 \times 10^{-6}\, x - 9 \times 10^{-5} \quad (2)$$

The coefficient of 1×10^{-10} in Equation 2 indicates that the period determined originally was about 0.7 second shorter than that determined in this work. The difference between the original period determined by Bruna (1930) and that determined from my data with a linear regression is also 0.7 second.

An (O–C) diagram for the years 2000 to 2015, based on the ephemeris in Equation 1, shows variations, although the differences are small and within the range of the average error of 0.016 day (Figure 2). However, there was an apparent sinusoidal trend in the O–C values from 2011 (epoch –3625) to 2015 (Figure 3). In 2015, the two very low O–C values of –0.002 and –0.0035 were due to minima in the I band and the other very low value of –0.002 was in the V band, yet the O–C values in other bands on those dates were not different from other sets in 2015.

There were variations in the magnitudes of the primary and secondary eclipse minima (Table 2) and in the amplitudes of the

Table 2. TW Cru times of minimum, observed minus calculated (O–C) differences in epochs, and photometric data.

*Year**	*Cycle*	*Epoch HJD*	*Error**	*O–C*	*Error*	*Band*	*Magnitude*	*Error*
1926[a]	–83281	2424776.15740		0.0353	0.0050			
2000[b]	–13476.5	2451870.32000		0.0000	0.0013	V		
2002[c]	–11853.5	2452500.27800		0.0003		V		
2004[d]	–10291	2453106.75300		0.0003		V		
2011	–3625.5	2455693.92413	0.00141	–0.0024	0.0014	V	12.80	0.006
2011	–3623	2455694.89528	0.00113	–0.0016	0.0012	V	12.85	0.006
2011	–3594.5	2455705.95682	0.00125	–0.0022	0.0013	V	12.80	0.007
2011	–3587	2455708.86768	0.00112	–0.0024	0.0012	V	12.85	0.007
2011	–3586.5	2455709.06123	0.00115	–0.0029	0.0012	V	12.81	0.007
2011	–3540.5	2455726.91681	0.00105	–0.0019	0.0011	V	12.78	0.009
2011	–3489	2455746.90585	0.00112	–0.0023	0.0012	V	12.86	0.005
2012	–2677	2456062.07976	0.00104	–0.0013	0.0011	V	12.86	0.005
2012	–2662	2456067.90247	0.00113	–0.0008	0.0012	V	12.87	0.005
2012	–2661.5	2456068.09679	0.00130	–0.0005	0.0013	V	12.84	0.005
2012	–2595	2456093.90897	0.00093	0.0001	0.0010	V	12.88	0.006
2012	–2579.5	2456099.92465	0.00118	–0.0005	0.0012	V	12.82	0.004
2012	–2551	2456110.98609	0.00122	–0.0012	0.0012	V	12.86	0.005
2013	–1788.5	2456406.94846	0.00146	0.0014	0.0015	V	12.81	0.007
2013	–1788	2456407.14136	0.00130	0.0002	0.0013	V	12.89	0.007
2013	–1775.5	2456411.99343	0.00155	0.0005	0.0016	V	12.80	0.009
2013	–1775	2456412.18664	0.00139	–0.0004	0.0014	V	12.89	0.009
2014	–974	2456723.09018	0.00045	–0.0002	0.0005	V	12.84	0.013
2014	–902	2456751.03599	0.00125	–0.0007	0.0013	V	12.86	0.009
2014	–897	2456752.97711	0.00124	–0.0003	0.0013	V	12.86	0.006
2014	–825	2456780.92308	0.00019	–0.0007	0.0003	V	12.85	0.015
2014	–824.5	2456781.11878	0.00190	0.0009	0.0019	V	12.80	0.014
2014	–822.5	2456781.89589	0.00150	0.0017	0.0015	V	12.80	0.014
2014	–822	2456782.08876	0.00140	0.0005	0.0014	V	12.82	0.011
2015	–13	2457096.09706	0.00104	0.0003	0.0011	V	12.89	0.004
2015	–13	2457096.09727	0.00137	0.0005	0.0014	I	11.86	0.006
2015	–0.5	2457100.94868	0.00122	0.0002	0.0012	V	12.83	0.004
2015	0	2457101.14310	0.00102	0.0005	0.0010	V	12.88	0.004
2015	2	2457101.91918	0.00120	0.0003	0.0012	I	11.97	0.006
2015	53.5	2457121.90481	0.00140	–0.0035	0.0014	I	11.80	0.006
2015	53.5	2457121.90820	0.00196	–0.0001	0.0020	V	12.80	0.006
2015	53.5	2457121.90880	0.00316	0.0005	0.0032	B	13.63	0.012
2015	54	2457122.10039	0.00302	–0.0020	0.0030	I	11.86	0.006
2015	54	2457122.10256	0.00179	0.0002	0.0018	B	13.71	0.012
2015	54	2457122.10302	0.00192	0.0007	0.0019	V	12.86	0.006
2015	95	2457138.01397	0.00160	–0.0023	0.0016	V	12.89	0.004
2015	95	2457138.01585	0.00173	–0.0004	0.0017	B	13.74	0.008
2015	100	2457139.95675	0.00275	–0.0002	0.0028	V	12.88	0.005
2015	100	2457139.95691	0.00179	–0.0001	0.0018	I	11.87	0.006
2015	100.5	2457140.15026	0.00175	–0.0008	0.0018	V	12.80	0.005
2015	100.5	2457140.15171	0.00189	0.0006	0.0019	I	11.80	0.006
2015	146.5	2457158.00564	0.00564	0.0000	0.0056	V	12.83	0.003
2015	146.5	2457158.00646	0.00224	0.0008	0.0022	B	13.67	0.007
2015	180	2457171.00805	0.00163	–0.0005	0.0016	I	11.96	0.009
2015	180	2457171.00856	0.00171	0.0001	0.0017	V	12.88	0.01

**Notes. Source: (a) Bruna 1930; (b) Pojmański 2002; (c) Kreiner 2004; (d) Dvorak 2004. Errors for epoch, O–C, and magnitudes, respectively, are shown for the present work.*

Table 3. Color indices and estimated spectral types and temperatures of the TW Cru component stars.

Parameter	*B–V*	*V–I*	*Spectral type*	*Teff (K)*
Maximum light	0.82 ± 0.01	0.87 ± 0.01	K0V	5280
Primary minimum	0.87 ± 0.01	0.92 ± 0.01	K2V	5040
Secondary minimum	0.86 ± 0.01	0.90 ± 0.02	K1V	5170

Table 4. Light curve model data used for the models shown in Figures 6 through 10. The convention used in BINARY MAKER 3 for W-type UMa systems, where the more massive star is the cooler component, is to invert the mass ratio.

Parameter	*General*	*Star 1*	*Star 2*
Mass ratio	1.5		
Fillout	0.11		
Inclination	70.8°		
Temperature (K)		5000	5170
Gravity coefficient		0.32	0.32
Limb darkening (V)		0.70	0.66
Limb darkening (I)		0.48	0.44
Limb darkening (B)		0.87	0.84

Table 5. Star spot parameters for the TW Cru light curve solutions in Figures 6 through 8. The Johnson V band fluxes were modeled, with an example of the solution in the I band for 2015-04-27. In each case, star 1 is the larger, cooler component.

Date and Passband	*Star*	*Co-Latitude*	*Longitude*	*Radius*	*Temperature factor*
2013-04-29 (V)	1	84	3	20	1.10
"	1	80	260	17	0.90
"	2	90	65	12	0.92
2015-03-19 (V)	1	70	135	18	0.93
"	2	60	200	22	0.96
2015-04-09 (V)	1	70	90	20	0.96
"	2	30	110	14	0.96
2015-04-09 (B)	1	70	90	20	0.96
"	2	30	110	14	0.96
2015-04-09 (I)	1	70	90	20	0.96
"	2	30	110	10	0.98
2015-04-27 (V)	1	80	112	20	0.86
"	1	70	200	24	0.96
"	2	55	112	24	0.86
2015-04-27 (I)	1	80	112	20	0.86
"	1	70	200	24	0.96
"	2	55	112	24	0.86

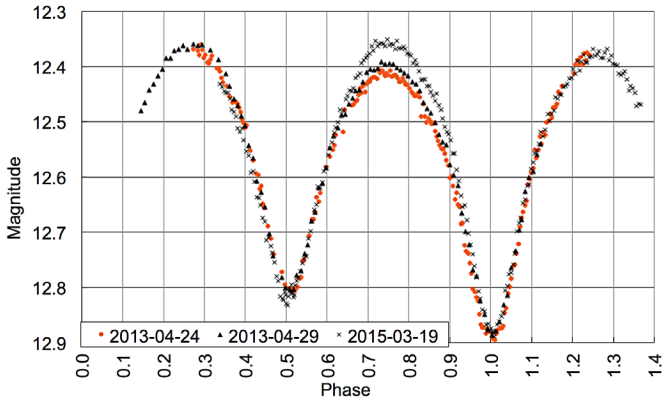

Figure 4. Phased light curves in the V passband demonstrating variations in eclipse amplitudes. The maximum magnitude was brighter after the primary minimum than after the secondary on 2013-04-24 and 2013-04-29. The maximum magnitude was brighter after the secondary minimum on 2015-03-19.

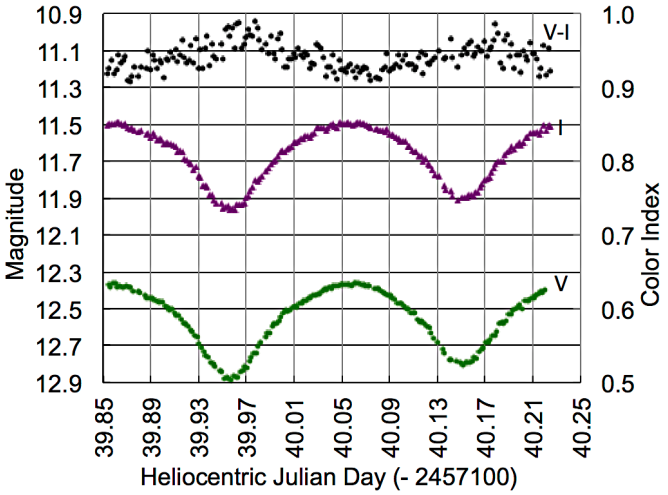

Figure 5. Light curves of TW Cru in V and I passbands (left Y axis) and the variation in color index (right Y axis) on 2015-04-27. The maximum magnitudes were similar after both the primary and secondary minima.

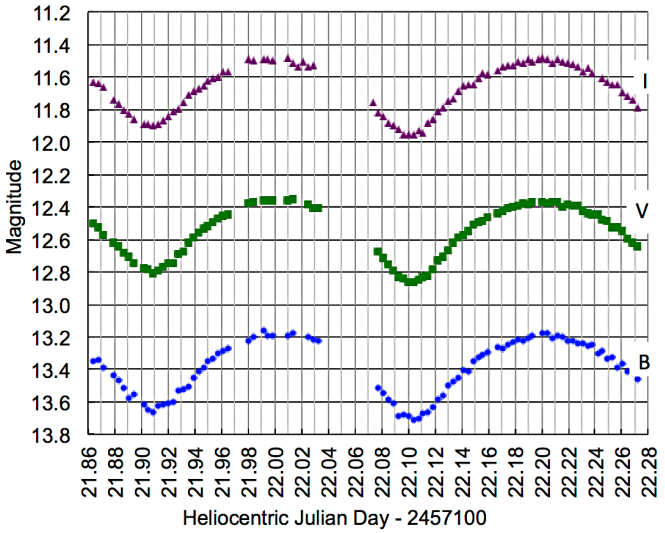

Figure 6. Light curves of TW Cru in B, V and I for 2015-04-09. The maximum magnitudes were similar after both the primary and secondary minima. The seeing was affected by a humid air mass and some cloud, which prevented the determination of accurate color indices.

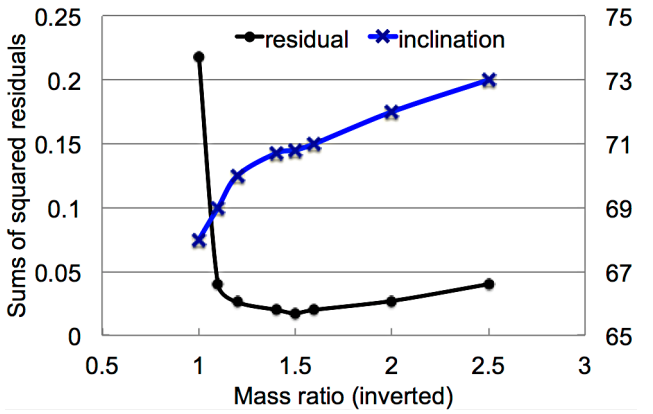

Figure 7. Selection of probable mass ratio with the q method: plot of the sum of squared residuals of the light curve fit (left axis) against a range of mass ratios. The inclination that gave the lowest residual value for each mass ratio is also shown (right axis).

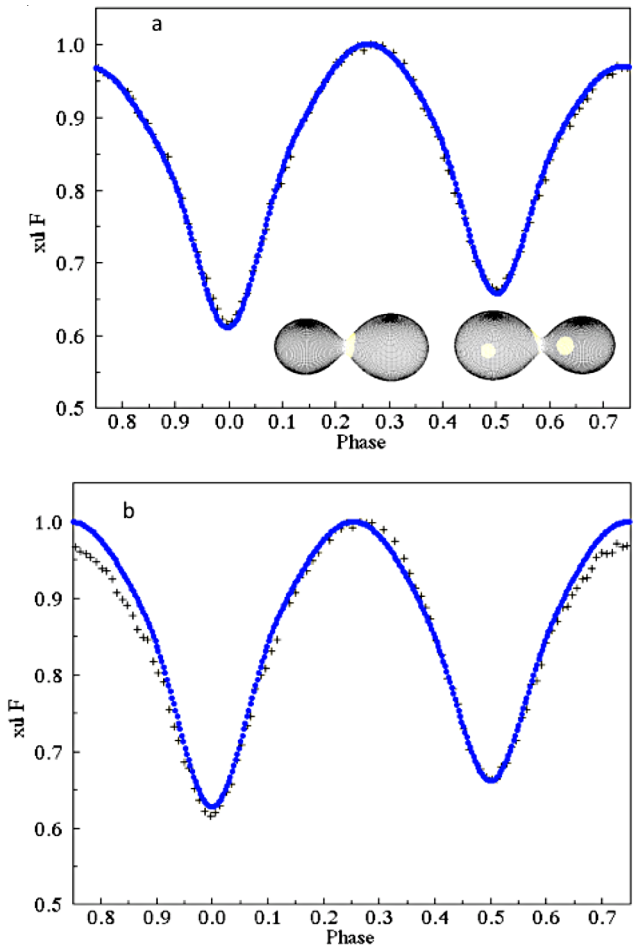

Figure 8. (a) Light curve (crosses) and best fit (blue line) of the V pass band for 2013-04-29. The average of residuals for the light curve fit was 0.006. Inset: the binary model at phases 0.25 (left) with a hot spot on star 1 at the point of contact and the positions of 2 cool spots at phase 0.75. Star 1 is the larger star, on the right at phase 0.25. (b) Light curve (crosses) and model (blue line) with the same parameters as in (a), but without spots.

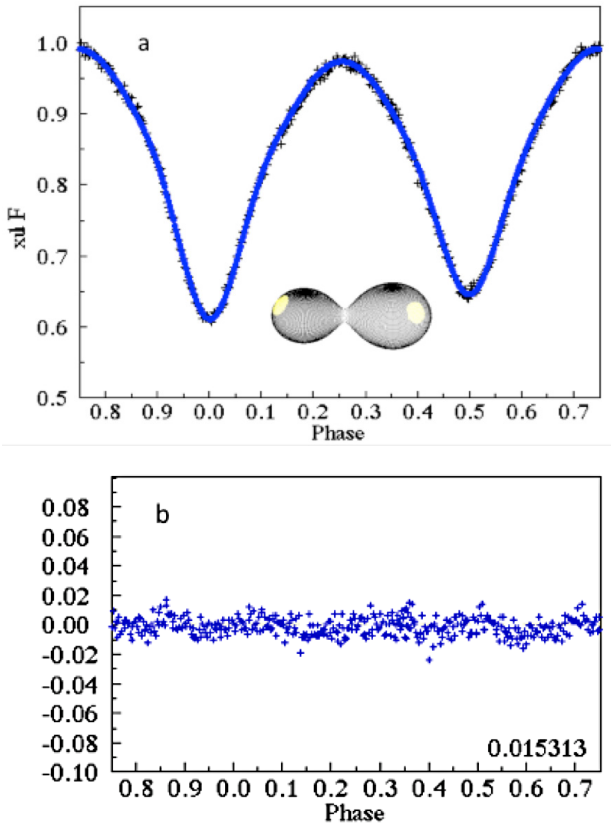

Figure 9. (a) Light curve (crosses) and best fit (blue line) of the V pass band for 2013-03-19 (epoch HJD 2457101.14310). The inset shows the spot positions on the binary at phase 0.25. (b) Residuals for the light curve plot (mean: 0.015).

eclipses. For example, the magnitude at maximum brightness between eclipses (phases 0.25 and 0.75) was brighter after the primary eclipses on some occasions, on 2013-04-24 (HJD 2456407.14136) and on 2013-04-29 (HJD 2456412.18664), for example, and it was brighter after the secondary eclipses at other times, on 2015-03-19 (HJD 2457100.94868), for example (Figure 4). In April 2015, the magnitudes at maximum brightness after both primary and secondary minima were similar (Figures 5 and 6). The color index was redder after the primary minimum than after the secondary and bluer at maximum light Figure 5).

3.2. Light curve modelling

As there are no spectral data available for TW Cru, the effective temperatures for modelling the light curves were estimated from the observed B–V and V–I color indices, which indicate the spectral types to be about K0 to K2 if there were no interstellar reddening (Table 3). The B–V value in the APASS database is 0.768, which indicates the spectral type may be G9 (Table 1). A range of values for the mass ratio, inclination, and fillout factor was tried and those that gave the best fit to the light curves, with the lowest sums of squared residuals of 0.006 for the light curve on 2013-04-29, are shown in Table 4. The "q method" was used to select a probable mass ratio (Figure 7). Star spots had to be included before good fits to the observed light curves were obtained; compare Figures 8a and 8b. Examples showing the variation in spot positions, size, and relative temperature are shown in Figures 8, 9, 10, and 11. The spot parameters are given in Table 5.

For a good fit, the astrophysical model of the light curve obtained in 2013-04-29 required the addition of a cool spot on each star and a hot "spot" at the zone of contact on the larger component (Figure 8a and Table 5). Two cool spots, one on each star, provided a good fit for modelling the light curve obtained on 2015-03-19 (Figure 9a and Table 5). An example of the graph of the residuals in the light curve model plot is shown in Figure 9b.

A comparison of the fitting of the model in the V bandpass to the light curves in the B and I bands is shown in Figure 10. Although there were some gaps in the light curve due to cloud, and poor seeing affected the signal to noise ratio, especially in the B band, the fit was good. Only a small adjustment was made to the spot size and temperature on star 2 in the I band. On 2015-04-27, three cool spots were required to provide a good fit, with two spots on the larger star and one on the smaller, hotter component (Figure 11a and Table 5). The model of the light curve in the I passband did not require a change in the relative temperatures of the spots (Figure 10c and Table 5).

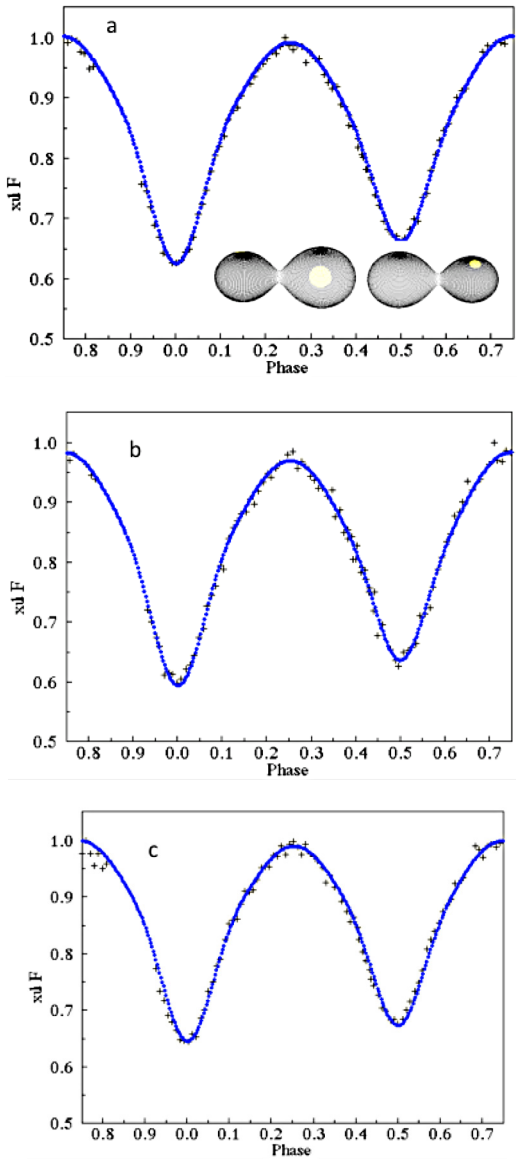

Figure 10. (a) Light curve (crosses) and best fit (blue line) of the V pass band for 2015-04-09; the mean of the residuals was 0.007. Inset: spot positions on the binary model at phases 0.25 and 0.75. (b) Light curve and best fit for the B pass band; mean of the residuals was 0.012. (c) Light curve and best fit for the I pass band; the mean of the residuals was 0.012.

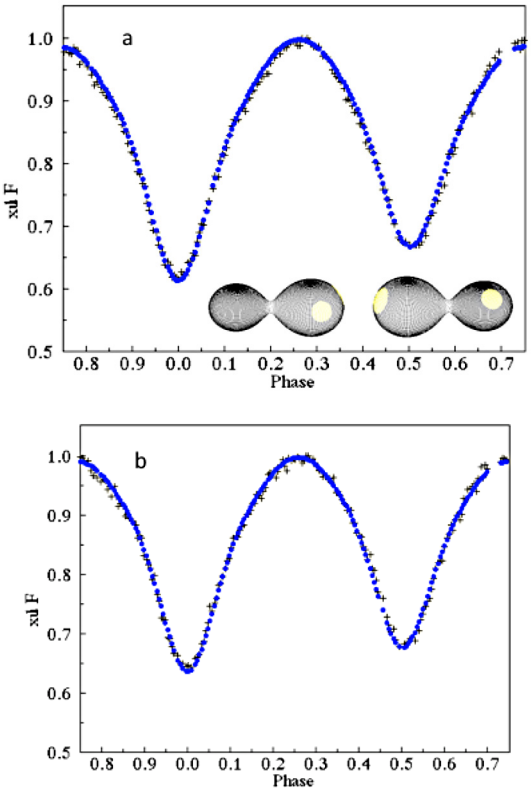

Figure 11. (a) Light curve (crosses) and best fit (blue line) of the V pass band for 2015-04-27. The mean of the light curve residuals was 0.014. Inset: spot positions on the binary model at phases 0.25 and 0.75. (b) Light curve (crosses) and best fit (blue line) of the I pass band. The mean of the light curve residuals was 0.012. Spot parameters were not changed (see Table 5).

4. Discussion

The period determined here is similar to that determined by Kreiner (2004) and differs by 0.7 second from the period derived originally by Bruna (1930). Note that the first epoch shown in Table 2 differs from that given in the *General Catalogue of Variable Stars* (GCVS; Kholopov, *et al.* 1985); the latter is in fact the epoch at phase 0.378 shown in Table 1 of Bruna (1930). As there are no data for times of minimum between 1926 and 2000, it is possible that the error stated for the original period was larger than that published and so there may not be any difference in the period.

The variability in times of minimum is probably due to asymmetry in the light curves; in particular, the rise from the minima to maximum light was slower than the decrease to minima on several occasions. Kwee (1958), in his study of eclipsing binaries using photoelectric photometry, concluded that very short term variations in the periods were due to asymmetry in the light curves, and not the effect of mass exchange. Some of the variability in the times of minimum could also be variability in the light curves due to poor seeing conditions, which was often the case in southeast Queensland where the wet season extends from January to April, the prime season for Crux.

As a quadratic equation could be fitted to the O–C curve for the 2011–2015 data, it is possible that the some of the year-to-year variation in the O–C values might be caused by the presence of a third component. However, a longer time series of observations is required to determine if that is the case. A more likely explanation for the apparent differences in O–C values over the 5-year period from 2011 to 2015 is that the formation and movement of star spots varies not only between cycles on a short term basis—over about 100 cycles—but also on a much longer term like the sunspot cycle on the Sun. Variations in the magnitudes and exact times of the maxima and minima of the light curves are probably caused by the movement of cool spots on the stars.

The spectral type may be earlier due to interstellar reddening, but as the distance of TW Cru is not known, the effect of reddening on color index cannot be determined. If it were severe, then the B–V value would indicate a spectral class a little later than that given by the V–I value, but in fact both

values agree with recent tabulated values for K0 and K2 dwarf stars (Pecaut and Mamajek 2013). However, these values are only a guide; the spectral types of the TW Cru stars could be earlier. Until spectral types and the mass ratio are determined spectroscopically, the models shown here are provisional. Their main value is in indicating that the short term variability in the light curves is probably due to cool star spots, which is what would be expected from magnetic activity in G or K type stars with very rapid rotation rates (Hilditch 2001). Hilditch (2001) discussed the problems in modelling contact binary stars with asymmetric light curves and commented that the placement of cool star spots over the surfaces can lead to ambiguous results; Doppler imaging and detailed eclipse mapping, together with photometry in several band passes and high resolution spectroscopy, are needed to improve our understanding of these systems.

Although the cool spots were sufficient to explain most variations in the light curves, a hot zone on the cooler star around the contact region gave the best fit to the model for 2013-04-29 (Table 5). The variation in color index from reddest (coolest) during the eclipses, particularly the primary eclipse, and bluer (hotter) at phases 0.25 and 0.75 suggests that the contact zone was, in general, hotter than other regions of the binary (Figure 5). There may be other solutions to the light curve with the incorporation of a hot contact zone, but until the mass ratio and spectral types are determined spectroscopically, further work on model parameters is not warranted.

5. Conclusions

There has been no substantial change in the period of TW Cru since its discovery in 1926. Small variations apparent in the times of minimum and asymmetry in the light curves are most likely due to the effect of cool star spots. Star spots were required to produce good fits to the light curves in preliminary astrophysical models prepared in BINARY MAKER 3. These indicate that the component stars are very active magnetically. Spectroscopic studies are needed for determining the spectral types and mass ratio of TW Cru.

6. Acknowledgements

I am grateful to Dr. Tom Richards for introducing me to the study of eclipsing binary stars and for his guidance and encouragement in photometry. I thank the referee, whose comments improved the presentation of this work. Some of the equipment was purchased with the aid of grants from the Edward Corbould Research Fund of the Astronomical Association of Queensland. This research made use of the VizieR catalogue access tool, the SIMBAD database, operated at CDS, Strasbourg, France, and the AAVSO Photometric All-Sky Survey (APASS), funded by the Robert Martin Ayers Sciences Fund.

References

Binnendijk, L. 1970, *Vistas Astron.*, **12**, 217.

Bradstreet, D. H. 2005, in *The Society for Astronomical Sciences 24th Annual Symposium on Telescope Science* (May 24–26, 2005), Society for Astronomical Sciences, Rancho Cucamonga, CA, 23.

Bradstreet, D. H., and Steelman, D. P. 2002, *Bull. Amer. Astron. Soc.*, **34**, 1224.

Bruna, P. P. 1930, *Bull. Astron. Inst. Netherlands*, **6**, 45.

Diffraction Limited. 2012, MAXIMDL image processing software (http://www.cyanogen.com).

Dvorak, S. W. 2004, *Inf. Bull. Var. Stars*, No. 5542, 1.

Henden, A. A., *et al.* 2013, AAVSO Photometric All-Sky Survey, data release 7 (http://www.aavso.org/apass).

Hilditch, R. W. 2001, *An Introduction to Close Binary Stars*, Cambridge Univ. Press, Cambridge.

Kholopov, P. N., *et al.* 1985, *General Catalogue of Variable Stars*, 4th ed., Moscow.

Kreiner, J. M. 2004, *Acta Astron.*, **54**, 207.

Kwee, K. K. 1958, *Bull. Astron. Inst. Netherlands*, **14**, 131.

Landolt, A. U. 2007, *Astron. J.*, **133**, 2502.

Mohajerani, S., and Percy, J. R. 2015, *J. Amer. Assoc. Var. Star Obs.*, **39**, 80.

Munari, U., Henden, A. A., Frigo, A., and Dallaporta, S. 2014, *J. Astron. Data*, **20**, 4.

Pecaut, M. J., and Mamajek, E. E. 2013, *Astrophys. J., Suppl. Ser.*, **208**, 9.

Pojmański, G. 2002, *Acta Astron.*, **52**, 397.

Pribulla, T., and Rucinski, S. M. 2006, *Astron. J.*, **131**, 2986.

Richards, T. 2013, Southern Eclipsing Binaries Programme of the Variable Stars South group (http://www.variablestarssouth.org/index.php/research/eclipsing-binaries).

Richards, T. 2015, private communication.

Thinking Man Software. 1992–2014, DIMENSION 4 software (http://www.thinkman.com/dimension4/).

Vanmunster, T. 2013, Light Curve and Period Analysis Software, PERANSO v.2.50 (http://www.peranso.com/).